bioRxiv preprint doi: https://doi.org/10.1101/094912; this version posted December 24, 2016. The copyright holder for this preprint (which was not certified by peer review) is the author/funder, who has granted bioRxiv a license to display the preprint in perpetuity. It is made available under a CC-BY-NC-ND 4.0 International license.

Title: Two loci contribute epistastically to heterospecific pollen rejection, a postmating isolating barrier between species

Jennafer A. P. Hamlin[1]

Natasha A. Sherman[1]

Leonie C. Moyle[1,*]

[1]Department of Biology, Indiana University, 1001 East Third Street, Bloomington, Indiana, USA, 47405

bioRxiv preprint doi: https://doi.org/10.1101/094912; this version posted December 24, 2016. The copyright holder for this preprint (which was not certified by peer review) is the author/funder, who has granted bioRxiv a license to display the preprint in perpetuity. It is made available under a CC-BY-NC-ND 4.0 International license.

Short Title: Epistasis for Postmating Prezygotic Isolation

Keywords: Epistasis, female choice, postmating prezygotic barriers, reproductive isolation, speciation, species barriers, unilateral incompatibility

*Correspondence should be sent to:

Leonie C. Moyle
Department of Biology, Indiana University,
1001 East Third Street,
Bloomington, Indiana, USA, 47405
(812) 856 - 7027
lmoyle@indiana.edu

bioRxiv preprint doi: https://doi.org/10.1101/094912; this version posted December 24, 2016. The copyright holder for this preprint (which was not certified by peer review) is the author/funder, who has granted bioRxiv a license to display the preprint in perpetuity. It is made available under a CC-BY-NC-ND 4.0 International license.

ABSTRACT

Recognition and rejection of heterospecific male gametes occurs in a broad range of taxa, although the complexity and redundancy of mechanisms underlying this postmating cryptic female choice is poorly understood. In plants, the arena for these interactions is the female reproductive tract (pistil), within which heterospecific pollen tube growth can be arrested via active molecular recognition. Unilateral incompatibility (UI) is one such pistil-mediated barrier in which pollen rejection occurs in only one direction of an interspecific cross. We investigated the genetic basis of pistil-side UI between *Solanum* species, with the specific goal of understanding the role and magnitude of epistasis between UI QTL. Using heterospecific introgression lines (ILs) between *Solanum pennellii* and *S. lycopersicum*, we assessed the individual and pairwise effects of three chromosomal regions (*ui1.1*, *ui3.1*, and *ui12.1*) previously associated with interspecific UI among *Solanum* species. Specifically, we pyramided *ui12.1* with each of *ui1.1* and *ui3.1*, and assessed the strength of UI pollen rejection in pyramided (double introgression) lines, compared to single introgression genotypes. We found that none of the three QTL individually showed UI rejection phenotypes, but lines combining *ui3.1* and *ui12.1* showed significant pistil-side pollen rejection. Furthermore, double introgression lines that combined different chromosomal regions overlapping *ui3.1* differed significantly in their rate of UI, consistent with at least two genetic factors on chromosome three contributing quantitatively to interspecific pollen rejection. Together, our data indicate that loci on both chromosomes 3 and 12 are jointly required for the expression of UI between *S. pennellii* and *S. lycopersicum* suggesting that coordinated molecular interactions among a relatively few loci underlying the expression of this postmating prezygotic barrier. In addition, in conjunction with previous data, at least one of these loci appears to also contribute to conspecific self-

bioRxiv preprint doi: https://doi.org/10.1101/094912; this version posted December 24, 2016. The copyright holder for this preprint (which was not certified by peer review) is the author/funder, who has granted bioRxiv a license to display the preprint in perpetuity. It is made available under a CC-BY-NC-ND 4.0 International license.

48 incompatibility, consistent with a partially shared genetic basis between inter- and intraspecific
49 mechanisms of postmating prezygotic female choice.
50

bioRxiv preprint doi: https://doi.org/10.1101/094912; this version posted December 24, 2016. The copyright holder for this preprint (which was not certified by peer review) is the author/funder, who has granted bioRxiv a license to display the preprint in perpetuity. It is made available under a CC-BY-NC-ND 4.0 International license.

INTRODUCTION

Traits that underpin sexual recognition and rejection can be critical both for mate choice within species and for prezygotic isolating barriers between species. Such traits can contribute to premating interactions, including behavioral and chemical signals that indicate appropriate mating partners, or can act after mating but before fertilization, including interactions between gametes and/or between gametes and an internal reproductive tract. In the latter case, the female reproductive tract can be an important arena in which these interactions play out (Bernasconi *et al.*, 2004). Many species are known to exhibit "cryptic female choice" in which genotype-specific interactions between male gametes and female tissues determine the paternity of offspring following mating with more than one male genotype (Alonzo *et al.*, 2016). Similarly, female choice can influence the outcome of mating between species, when females are able to recognize and reject heterospecific male gametes. The specific mechanisms, by which this choice is exercised, either within or between species, have been identified in some select systems (Price, 1997; Manier *et al.*, 2013; Castillo and Moyle, 2014) and see also below). However, much remains to be understood about the complexity and redundancy of these postmating prezygotic female traits, the specific loci that are necessary and sufficient for recognition and rejection, and the extent to which these mechanisms are shared between intraspecific and interspecific sexual interactions.

Plants are among the many sexually reproducing organisms able to recognize and reject gametes from their own and other species. In angiosperms, recognition and rejection of pollen can occur at several stages after pollen is transferred (e.g. via wind or animal vectors) to the female receptive stigma (the receiving tissue for pollen deposition), including during pollen

bioRxiv preprint doi: https://doi.org/10.1101/094912; this version posted December 24, 2016. The copyright holder for this preprint (which was not certified by peer review) is the author/funder, who has granted bioRxiv a license to display the preprint in perpetuity. It is made available under a CC-BY-NC-ND 4.0 International license.

74 germination and pollen tube growth (via cell growth/elongation) down the female style (the
75 reproductive tract that connect the stigma to the ovary). These 'pollen-pistil' interactions (the
76 pistil is composed of the stigma and style) are roughly equivalent to post-copulatory interactions
77 in animals, with the exception that pollen tubes (male gametophytes) actively express a
78 substantial fraction of their own genome (Rutley and Twell, 2015). Molecular mechanisms of
79 pistil-mediated recognition and rejection of conspecific pollen tubes are arguably best
80 understood in the context of genetic self-incompatibility (SI), whereby pollen from self or close
81 relatives is recognized and rejected in the female style. Intraspecific SI is mediated by the '*S*-
82 locus' which encodes (at least) two molecules responsible for the self-rejection mechanism: an *S*-
83 *RNase* (the female/stylar component) that recognizes one or more pollen-expressed F-box
84 protein(s) in germinated pollen tubes, and arrests pollen tube growth within the style. In
85 gametophytic SI systems, pollen is rejected in styles when it bears an *S*-allele that is identical to
86 an *S*-allele of the pistil (maternal) parent (McClure *et al.*, 1989). Because individuals will always
87 share *S*-alleles with themselves, this genetic system prevents self-fertilization when pollen is
88 transferred within a flower or between flowers on the same individual. In addition to genes at
89 the *S*-locus, other factors are also known to be required for SI function, including HT—a small
90 asparagine-rich protein (McClure *et al.*, 1999)—and other stylar glycoproteins (McClure *et al.*,
91 2000; Cruz-Garcia *et al.*, 2003; Hancock *et al.*, 2003; de Graaf, 1999) on the pistil-side, and
92 pollen-side proteins including Cullins that are components of pollen protein complexes (Zhao *et*
93 *al.*, 2010; Li and Chetelat, 2014; Hua and Kao, 2006). SI genotypes can give rise to SC lineages
94 when one or more of these molecular components has a loss-of-function mutation(s)
95 (Charlesworth and Charlesworth, 1979; Mable, 2008; Stone, 2002; Takayama and Isogai, 2005;
96 Tao and Iezzoni, 2010; Covey *et al.*, 2010).

bioRxiv preprint doi: https://doi.org/10.1101/094912; this version posted December 24, 2016. The copyright holder for this preprint (which was not certified by peer review) is the author/funder, who has granted bioRxiv a license to display the preprint in perpetuity. It is made available under a CC-BY-NC-ND 4.0 International license.

97 Pistil-mediated pollen tube rejection can also act as an important species barrier among
98 plant lineages, especially those that are otherwise weakly isolated by trait differences associated
99 with premating (e.g. pollinator or flowering time) isolation. In comparison to SI pollen-pistil
100 interactions, the molecular basis of recognition and rejection of heterospecific pollen is less well
101 understood. Nonetheless, in several cases there is strong evidence that elements of this behavior
102 are mechanistically associated with SI. Classical studies of interspecific pollen-pistil barriers in
103 some species groups indicate that these are often observed between lineages that differ in the
104 presence/absence of SI, such that SI species styles reject pollen from self-compatible (SC)
105 species, but the reciprocal cross does not show stylar rejection (the so-called "SI x SC rule"; de
106 Nettancourt, 1997; Bedinger *et al.*, 2011; Lewis and Crowe, 1958; Murfett *et al.*, 1996).
107 Molecular and functional analysis of the resulting "unilateral incompatibility" (UI) has
108 confirmed that genetic components of SI can be shared in part with those of UI. For example, in
109 some *Nicotiana* species, transforming non-rejecting SC genotypes with a functional *S-RNase* can
110 be sufficient to confer the ability to reject pollen from other SC species (Hancock *et al.*, 2003).
111 Additional factors required for SI can also play a role in stylar (female)-side UI. For example,
112 both *S-RNase* and HT protein are required for SI *Nicotiana alata* rejection of pollen from SC *N.*
113 *plumbaginifolia*; normal *S-RNase* expression is individually insufficient (Hancock *et al.*, 2003;
114 McClure *et al.*, 1999). Similarly, in *Solanum* co-transformation of functional copies of both HT
115 and *S-RNase* into SC species *S. lycopersicum* is sufficient to confer the ability to reject pollen
116 from other SC species (Tovar-Méndez *et al.*, 2014).
117
118 While these observations clearly indicate that SI-associated molecular mechanisms can
119 be sufficient to enable pistil-side pollen rejection between species, other data indicate that these

bioRxiv preprint doi: https://doi.org/10.1101/094912; this version posted December 24, 2016. The copyright holder for this preprint (which was not certified by peer review) is the author/funder, who has granted bioRxiv a license to display the preprint in perpetuity. It is made available under a CC-BY-NC-ND 4.0 International license.

120 mechanisms are more complex in nature. In particular, there is also evidence for *S-RNase*-
121 independent UI mechanisms (Murfett *et al.*, 1996), often from species pairs that exhibit UI, but
122 do not follow the SI x SC rule. For example, in *Solanum*, some SC populations of *S. pennellii*
123 and *S. habrochaites* lack *S-RNase* expression but continue to be competent to reject interspecific
124 pollen from SC species (Covey *et al.*, 2010; Baek *et al.*, 2015; Chalivendra *et al.*, 2013). Less
125 directly, QTL mapping between *Solanum* species that both differ in SI-status and show UI, have
126 detected UI QTL that do not colocalize with the *S*-locus. An analysis between SI *S. habrochaites*
127 and SC *S. lycopersicum* detected three UI QTL, only one of which was localized to the *S*-locus
128 (Bernacchi and Tanksley, 1997). A second study between SI *S. pennellii* and SC *S. lycopersicum*
129 detected two UI QTL, neither of which was at the *S*-locus (Jewell, 2016). Interestingly, the two
130 non-*S*-locus QTL detected in these studies (*ui3.1*, *ui12.1*) both localize to the same genomic
131 regions on chromosomes 3 and 12, suggesting a common genetic basis for UI among different
132 species. Moreover, in both studies, one of these QTL (*ui12.1*) co-localized with the known
133 genomic location of HT, and in one case (Jewell, 2016) the presence/absence of HT expression
134 in mature styles was significantly associated with the phenotypic strength of UI.
135
136 Overall, these data suggest that there might be substantial overlap between molecular
137 mechanisms of SI and UI, including both *S-RNase*-dependent or -independent mechanisms, but
138 also involvement of additional loci that have yet to be molecularly identified, and whose
139 relationship to SI is unknown. As such, several important aspects of the genetics of pistil-side UI
140 remain unclear, including the minimum number of factors sufficient to express *S-RNase*-
141 independent UI, the degree of overlap with molecular loci underpinning *S-RNase*-dependent

bioRxiv preprint doi: https://doi.org/10.1101/094912; this version posted December 24, 2016. The copyright holder for this preprint (which was not certified by peer review) is the author/funder, who has granted bioRxiv a license to display the preprint in perpetuity. It is made available under a CC-BY-NC-ND 4.0 International license.

142 mechanisms, and therefore the level of redundancy between alternative mechanisms underlying
143 these important postmating forms of female mate choice.
144
145 Here our goal was to assess the specific role of three chromosomal regions in affecting
146 pistil-side UI between species. Focusing on the UI QTL previously identified in two different
147 Solanum species crosses—*ui1.1*, *ui3.1*, and *ui12.1* (Bernacchi and Tanksley, 1997; Jewell,
148 2016)—our aim was to evaluate the individual and joint effects of these three unlinked
149 chromosomal regions on the expression of UI. To do so, we used near isogenic lines (NILs), in
150 which single chromosomal regions from a donor species genotype (*Solanum pennellii)* are
151 introgressed into the genetic background of an otherwise isogenic recipient species (*Solanum*
152 *lycopersicum*). Lines incorporating three different introgressed regions (from chromosomes 1, 3,
153 and 12) were examined individually and in pairwise combinations; the latter double introgression
154 lines (DILs: Canady *et al.* 2006 ; sometimes called 'pyramid lines': Gur and Zamir, 2004) were
155 created via crosses among NILs (see Methods). Two criteria were used to evaluate evidence for
156 epistasis between these target loci. First, we examined evidence for transmission ratio distortion
157 (TRD) in the products of crosses between different NILs, to look for evidence that particular
158 genotypes were over- or underrepresented. Second, we quantified the strength of pistil-side UI
159 response phenotypes in the DIL lines and compared this to the same phenotype in single (NIL)
160 introgression genotypes. This comparison allowed us to evaluate whether the quantitative effects
161 of individual introgressions differs in the presence of a second introgressed locus, and to evaluate
162 the minimum number of loci required to express pistil-side interspecific pollen rejection. We find
163 evidence that loci on chromosomes 3 and 12 are simultaneously required in order to express UI;
164 lines in which these loci are represented individually are unable to reject heterospecific pollen.

bioRxiv preprint doi: https://doi.org/10.1101/094912; this version posted December 24, 2016. The copyright holder for this preprint (which was not certified by peer review) is the author/funder, who has granted bioRxiv a license to display the preprint in perpetuity. It is made available under a CC-BY-NC-ND 4.0 International license.

One of these QTL—*ui12.1*—likely involves a known molecular contributor to SI (HT protein) thus further supporting the inference that factors associated with SI contribute to the expression of the UI phenotype. In addition, comparisons among DILs created using overlapping sections of *ui3.1* suggest that this other QTL might be underpinned by at least two separate genetic factors that additively contribute to the genetic variation in the strength of UI.

METHODS

Study System:

The tomato clade (Solanum section Lycopersicon) contains 13 closely-related species known to be separated by a range of incomplete pre- and postzygotic isolating barriers (Moyle, 2008), including pollen-pistil incompatibility, and specifically UI (Bedinger *et al.*, 2011; Covey *et al.*, 2010). Baek *et al.* (2015) directly examined the strength of pollen tube rejection between all 13 species within the tomato clade and found evidence that UI was strongest and most consistently observed between SI x SC species. Among other genetic mapping resources in this group are several introgression line libraries in which chromosomal regions representing most or all of a donor species genome have been serially introgressed into the genetic background of a recipient species, usually the domesticated tomato *S. lycopersicum* (Bernacchi and Tanksley, 1997; Eshed and Zamir, 1995). For this study, we used lines drawn from a NIL library previously developed between *S. pennellii*, a wild tomato species, and S. *lycopersicum*, where each line contains a marker delimited homozygous region of *S. pennellii* accession LA0716 introgressed into the genomic background of *S. lycopersicum* accession LA3475 (Eshed *et al.*, 1992; Eshed and Zamir, 1995; Eshed and Zamir, 1994). We used four different lines drawn from this library (Supplemental Table 1). IL1-1 overlaps the genomic location of the *S*-locus as well as

bioRxiv preprint doi: https://doi.org/10.1101/094912; this version posted December 24, 2016. The copyright holder for this preprint (which was not certified by peer review) is the author/funder, who has granted bioRxiv a license to display the preprint in perpetuity. It is made available under a CC-BY-NC-ND 4.0 International license.

188 the location of *ui1.1*, the UI locus previously mapped in an F2 population between *S.*
189 *lycopersicum* and *S. habrochaites* (Bernacchi and Tanksley, 1997). IL3-3 and IL3-4 contain *S.*
190 *pennellii* introgression regions that overlap the previously mapped *ui3.1* in (Bernacchi and
191 Tanksley, 1997) and in (Jewell, 2016), which together spans a broad genomic region (~70 cM);
192 these lines contain an overlapping region of approximately 44 cM (Supplemental Figure 1).
193 IL12-3 overlaps the previously mapped *ui12.1* in prior studies (Bernacchi and Tanksley, 1997).
194 Note that the known chromosomal location of HT protein falls within both IL12-3 and
195 *ui12.1*. HT was duplicated in the ancestor of Solanum, resulting in two tandemly arrayed
196 paralogs (HT-A and HT-B) at this chromosome 12 location (Covey *et al.*, 2010). Moreover, both
197 HT-A and HT-B are expressed in *S. pennellii* LA0716 but are non-functional in *S. lycopersicum*
198 due to null mutations in both HT-A and HT-B (Kondo *et al.*, 2002; Covey *et al.*, 2010). In
199 contrast, the *S-RNase* protein at the *S*-locus is non-functional in both *S. pennellii* and *S.*
200 *lycopersicum* genotypes in this experiment; *S. pennellii* is normally an SI species, but SI has
201 recently been lost in this population due to a complete loss of the *S-RNase* gene
202 (Solyc01g055200) (Li and Chetelat, 2015). Therefore we included an IL spanning *ui1.1* here in
203 order to assess whether other genes contained within this chromosomal region also contribute to
204 *S-RNase*-independent mechanisms of UI.
205
206 **Construction of Double Introgression Lines:**
207 Seeds for our four target introgression lines were obtained from the Tomato Genetics
208 Resource Center (tgrc.ucdavis.edu). To generate lines with two introgressed *S. pennellii* regions
209 (Double Introgression Lines, or DILs), crosses were performed pairwise between NIL lines
210 (Table 1), and resulting heterozygous F_1s were then selfed to generate F_2 seeds (a 'DIL

bioRxiv preprint doi: https://doi.org/10.1101/094912; this version posted December 24, 2016. The copyright holder for this preprint (which was not certified by peer review) is the author/funder, who has granted bioRxiv a license to display the preprint in perpetuity. It is made available under a CC-BY-NC-ND 4.0 International license.

211 population') for genotyping and ultimately phenotyping. In this experiment, three different DIL
212 combinations were generated (Table 1) in which we combined *ui12.1* with *ui1.1* and with the
213 two alternative (overlapping) *S. pennellii* regions at *ui3.1*. We were unable to generate offspring
214 from reciprocal crosses in all pairwise NIL-NIL combinations, as some of these did not produce
215 seeds in one of the crossing directions despite numerous attempts, or failed to produce viable
216 seed that was homozygous for target *S. pennellii* introgressions across each target QTL region.
217 Patterns of marker representation and segregation distortion in F2 progeny from the crosses are
218 discussed further below.
219
220 **Genotyping and Scoring Individuals:**
221 Progeny were genotyped within each F2 'DIL population' in order to identify individuals
222 that were homozygous for each *S. pennellii* introgression region and to describe patterns of
223 marker transmission ratio distortion (TRD) at these introgressions. These genotypes were used to
224 identify individuals that were homozygous at both introgression regions, for further phenotypic
225 assessment. Genotypes were also used to calculate overall genotype frequencies in segregating
226 populations, to assess if there was evidence of non-Mendelian patterns of transmission that might
227 be consistent with selection against certain genotypic combinations.
228 Genomic DNA was extracted using a modified CTAB protocol and Cleaved Amplified
229 Polymorphic Sequence (CAPS) genotyping was used to characterize the allelic identity (*S.*
230 *lycopersicum*: L or *S. pennellii*: P) using the target markers (Supplemental Table 2). CAPS
231 markers are restriction fragment variants caused by single nucleotide polymorphisms or
232 insertion/deletions, which create or abolish restriction enzyme recognition sites. Here we

bioRxiv preprint doi: https://doi.org/10.1101/094912; this version posted December 24, 2016. The copyright holder for this preprint (which was not certified by peer review) is the author/funder, who has granted bioRxiv a license to display the preprint in perpetuity. It is made available under a CC-BY-NC-ND 4.0 International license.

identified and genotyped markers that were designed to distinguish *S. lycopersicum* and *S. pennellii* alleles.

For each individual, DNA was amplified using PCR primers for each target marker and checked with gel electrophoresis. For each individual at each marker locus, a subsample of the amplicon was incubated with the relevant restriction endonucleases, and the digestion products were separated on 1.5% agarose gels, visualized with Ethidium Bromide staining, and imaged prior to manual scoring. Markers were chosen such that an allele from one parent would yield unique sized fragments (in bp) and the allele from the other parent would yield fragments of a different size (Supplemental Table 2). Thus each F_2 individual could be scored as homozygous for a parental allele (either *S. lycopersicum* or *S. pennellii*) at each marker, or as heterozygous in the case where the sample had the cleaved banding patterns representative of both parental alleles (Supplemental Table 2).

Each F_2 individual was genotyped at 2-4 markers associated with the chromosomal region they were expected to carry. For each target introgression on chromosomes 1 and 12, three markers were selected to span the length of the *S. pennellii* introgressed region. At the chromosome 3 locus, 5 markers in total were used for genotyping: three were located in the region shared between IL3-3 and IL3-4, and one each was located in the region exclusive to either IL3-3 or IL3-4. Each individual was scored as a homozygous *S. lycopersicum* (LL), heterozygous (LP), or homozygous *S. pennellii* (PP) genotype for each chromosomal region based on these marker genotypes. During the generation of DILs, recombination events could occur within the introgression *S. pennellii* region within each line, so scoring LL, LP, and PP individuals at each locus required some additional criteria. In particular, individuals were classified into genotypic categories based on the identity (L vs. P) of the majority of markers

bioRxiv preprint doi: https://doi.org/10.1101/094912; this version posted December 24, 2016. The copyright holder for this preprint (which was not certified by peer review) is the author/funder, who has granted bioRxiv a license to display the preprint in perpetuity. It is made available under a CC-BY-NC-ND 4.0 International license.

scored within each target regions. For example on IL3-3 if three of the four markers were PP and one marker was heterozygous (LP), this individual was scored as double homozygous for *S. pennellii* (PP) at this chromosomal region. For IL 12 -3, if the three markers within the introgressed region disagreed, marker 74.00 was used as the tiebreaker as this marker is physically close to the genomic location of HT-A and HT-B. For each DIL population, genotype frequencies at both loci (e.g. chromosome 3 and 12) were determined by combining data from the two chromosomal regions to calculate observed two-locus genotype frequencies.

Quantifying the presence and speed of UI:

To determine pollen tube growth phenotypes in each of our NIL and DIL lines, and therefore the phenotypic expression of UI, we used an assay in which pollen is manually applied to a target stigma, allowed to germinate and grow in styles for 24 hours, and then styles are fixed and stained to visualize and measure the extent of pollen tube growth (Figure 1). Evidence of UI is demonstrated via rejection of pollen tubes in the female reproductive tract (style), quantified in terms of the proportional distance of pollen tube growth out of the total style length—a value that can vary between zero (very rapid rejection at the top of the style) to 1 (complete pollen tube growth down the entire length of the style).

For each assay, an unopened bud was emasculated (1 day prior to opening) by removing the entire anther cone using hand forceps. Hand pollination was performed the following day, using *S. lycopersicum* (accession LA3475) pollen. This accession is the *S. lycopersicum* genomic background in our NILs and DILs; its pollen is expected to be rejected in a style that has an *S. pennellii*-derived genotype sufficient to mount a UI response. At 24 hours post-pollination, styles were collected into a 3:1 mixture of 95% EtOH:Glacial Acetic Acid in individual eppendorf

bioRxiv preprint doi: https://doi.org/10.1101/094912; this version posted December 24, 2016. The copyright holder for this preprint (which was not certified by peer review) is the author/funder, who has granted bioRxiv a license to display the preprint in perpetuity. It is made available under a CC-BY-NC-ND 4.0 International license.

tubes, and stored in the -20 freezer until imaging. 24 hours is more than sufficient for normal pollen tube growth down the complete length of the style, except when a UI response has been mounted. Pollination protocols were identical for both our NIL and DIL lines. We assayed 3 – 5 styles (technical replicates) per biological individual (Table 1).

To score pollen tube growth phenotypes, collected styles were placed in 5M NaOH and allowed to soften for 20 – 24 hours. Following softening, styles were washed and stained using 200 µL of Aniline blue fluorochrome for 3.5 hours in the dark, as described previously (Bedinger *et al.*, 2011; Jewell, 2016). Styles were then imaged using EVOS FL microscope with the DAPI setting. Stained pollen tubes fluoresce under these conditions, allowing us to differentiate style tissue from pollen tubes, and therefore determine the extent of pollen tube growth in each style. Because styles are generally too long to be captured in a single image, multiple images of the style were taken at 4x magnification and then stitched together using the program AutoStitch (Brown and Lowe, 2007). Images were visualized for measurement using ImageJ (Schneider *et al.*, 2012). Measurements taken on each style included 1) length of the style, 2) the "front" of the pollen (where the majority of the pollen stops in the style), and 3) the five longest pollen tubes. The average of the five pollen tubes was taken as our measurement of absolute distance traveled within this style, and UI was quantified as the proportional distance of pollen tube growth out of the total style length.

Statistical analyses:

To determine whether our observed genotypic frequencies significantly deviated from expected genotype frequencies in each 'DIL population', we calculated the expected proportion of each genotype and then performed a binomial test with a Bonferroni correction (Table 2). For

bioRxiv preprint doi: https://doi.org/10.1101/094912; this version posted December 24, 2016. The copyright holder for this preprint (which was not certified by peer review) is the author/funder, who has granted bioRxiv a license to display the preprint in perpetuity. It is made available under a CC-BY-NC-ND 4.0 International license.

each pairwise combination of loci, we used the upper and lower 95% confidence intervals around the regression coefficient to verify that the differences for genotypic classes were significant. We then performed planned independent contrasts for two different types of comparisons. Specifically, we asked 1) are DILs different from their parental NILs in terms of pollen tube growth and 2) are DILs different from each other? All analyses were run in RStudio version 0.99 (RStudio Team, 2015).

Data availability:

Introgression lines are available from the Tomato Genetics Resources Center (tgrc.ucdavis.edu). Marker information and phenotype data are supplied as supplementary material to the paper (Supplemental Table 1 and 2).

RESULTS

Departure from Mendelian Segregation Ratios:

We observed significant TRD in the DIL populations generated from crosses between different NILs (Table 2A, B, C), suggesting that there are interactions among alleles at these loci that specifically affect the likelihood of transmission of different introgression combinations. For example, a strong deviation in our IL3-3 and IL12-3 population is due to overrepresentation of homozygotes for *S. pennellii* alleles at both chromosomal regions, as well as overrepresentation of individuals that are heterozygous (LP) on chromosome 3 and homozygous (PP) on chromosome 12. This observed pattern of TRD is consistent with selection against *S. lycopersicum* alleles on a heterozygous F1 pistil (that has one allele at each of these two *S. pennellii* regions) (Figure 2). While some genotypes within the other DIL combinations deviate

bioRxiv preprint doi: https://doi.org/10.1101/094912; this version posted December 24, 2016. The copyright holder for this preprint (which was not certified by peer review) is the author/funder, who has granted bioRxiv a license to display the preprint in perpetuity. It is made available under a CC-BY-NC-ND 4.0 International license.

somewhat from the expected ratios (Table 2B and 2C), only two additional comparisons survived Bonferroni correction: in the DIL 12-3 x 3-4 combination, we found evidence of underrepresentation of homozygotes for *S. pennellii* (PP) alleles at chromosome 12, specifically when heterozygous (LP) on chromosome 3. Similarly, in DIL 1-1 x 12-3, genotypes homozygous for *S. pennellii* (PP) at chromosome 1 and heterozygous (LP) at chromosome 12 were significantly underrepresented.

UI phenotypes are observed in pairwise genotype combinations of ui3.1 with ui12.1:

We found that, while individual NIL lines showed no UI response, several DIL genotype combinations exhibited significant UI (Supplemental Figure 2). The proportion of pollen tube growth down the style in the NILs ranged from 0.93 – 0.98, with confidence intervals that overlapped 1.00, indicating pollen tubes that have grown the entire length of the style and reached the ovary (Table 1, Figure 3). In addition, the 95% confidence intervals on each NIL mean overlap, consistent with no differences among NILs in their UI phenotype (Figure 3). In comparison, mean pollen tube growth was generally reduced in the DIL genotypes and more highly variable between them (0.54 – 0.85; Table 1). Of these DIL combinations, two show evidence for significant reductions in proportional pollen tube growth, consistent with a quantitative UI response; both these DILs involve combinations of *S. pennellii* alleles on chromosomes 3 and 12 (i.e. IL3-3 or IL3-4 with IL 12-3). Planned independent contrasts confirmed that DILs which combine *S. pennellii* alleles on chromosomes 3 and 12 were significantly different from their respective NIL parental genotypes. (DIL12-3 x 3-3: $F_{1, 6}$ = 15.21; P = 0.0007, DIL 3-4 x 12-3: $F_{1, 6}$ = 30.21; P = 1.6e-05). In comparison, the DIL combining *S. pennellii* alleles on chromosomes 1 and 12 was not significantly different than its

bioRxiv preprint doi: https://doi.org/10.1101/094912; this version posted December 24, 2016. The copyright holder for this preprint (which was not certified by peer review) is the author/funder, who has granted bioRxiv a license to display the preprint in perpetuity. It is made available under a CC-BY-NC-ND 4.0 International license.

parental NILs ($F_{1,6} = 2.226$; $P = 0.1500$), and its 95% confidence intervals overlapped with the parental NIL genotypes, consistent with no significant interaction giving rise to a UI response in this DIL.

Patterns of pollen rejection suggest two loci underlie UI QTL on chromosome 3:

In addition to displaying significant UI phenotypes, we also found that the quantitative strength of UI differed significantly between DILs with chromosome 3 *S. pennellii* alleles, depending upon which specific chromosome 3 introgression they contained (12-3 x 3-3 versus 3-4 x 12-3: $F_{1,6} = 12.835$; $P = 0.0017$). In particular, DIL individuals carrying the *S. pennellii* alleles from IL3-3 showed a more rapid UI response (pollen tube growth arrests half way down the style) in comparison to DIL individuals carrying the *S. pennellii* alleles from IL3-4 (Figure 3A). These alternative DILs carry chromosome 3 introgressions that overlap by 44 cM (Supplemental Figure 1) as well as unique *S. pennellii* regions of 12 cM and 14 cM in IL3-3 and IL3-4 respectively, so the differences in UI phenotype between them could be explained by allelic differences within these unique regions. While there are several possible genetic interpretations of our observed patterns, the most parsimonious explanation requires only two loci at which *S. pennellii* alleles contribute to the quantitative expression of UI (in combination with *ui12.1*). The first locus (*ui3.1.1*) is contained within the chromosomal region shared between IL3-3 and IL3-4 and contributes an average effect of 0.19 micrometers to the quantitative strength of UI (see Figure 3B). In addition, the IL3-3 region contains a second locus, which, in combination with *ui3.1.1* and *ui12.1*, contributes an additional average effect of 0.23 micrometers to the quantitative strength of UI (see Figure 3B) when homozygous for *S. pennellii* alleles.

bioRxiv preprint doi: https://doi.org/10.1101/094912; this version posted December 24, 2016. The copyright holder for this preprint (which was not certified by peer review) is the author/funder, who has granted bioRxiv a license to display the preprint in perpetuity. It is made available under a CC-BY-NC-ND 4.0 International license.

DISCUSSION

While data suggest that there might be substantial overlap between molecular mechanisms of SI and UI, including both *S-RNase*-dependent or -independent mechanisms, several important aspects of the genetics of pistil-side UI remain unclear, including the minimum number of factors sufficient to express *S-RNase*-independent UI, the degree of overlap with molecular mechanisms underpinning *S-RNase*-dependent mechanisms, and therefore the level of redundancy between alternative mechanisms underlying these important postmating mechanisms of female mate choice. Here, our goals were to evaluate the minimum number of loci required to express pistil-side interspecific *S-RNase*-independent UI and evaluate the relative contribution of three different chromosomal regions to this phenotype. To do so, we examined the individual and combined (epistatic) effects of three candidate loci, pyramided as double introgression lines, on the expression of pistil-side pollen rejection. We find evidence that factors on both chromosomes 3 and 12 are jointly required for the expression of *S-RNase*-independent UI, whereas these loci have no effect individually. In addition, we find evidence consistent with gametophytic selection against certain genotypes, in the form of transmission ratio distortion. Together, these results suggest a strong role for the joint (epistatic) action of relatively few loci in determining the expression of pollen-pistil compatibility in this system.

Two loci are jointly required to express S-RNase independent UI between species:

Our findings clearly support a strong role for interactions between >1 molecular factor in the expression of *S-RNase*-independent UI. Specifically, we show that *S. pennellii* alleles from both chromosome 3 and 12 are necessary (and sufficient) for the expression of quantitative pistil-side UI against SC *S. lycopersicum* pollen. This confirms the general expectation that pollen

bioRxiv preprint doi: https://doi.org/10.1101/094912; this version posted December 24, 2016. The copyright holder for this preprint (which was not certified by peer review) is the author/funder, who has granted bioRxiv a license to display the preprint in perpetuity. It is made available under a CC-BY-NC-ND 4.0 International license.

394 recognition and rejection requires coordinated molecular interactions between several proteins,
395 consistent with other kinds of molecular recognition and rejection mechanisms (McClure *et al.*,
396 1999; McClure *et al.*, 2000), but also indicates that the products of relatively few loci are
397 sufficient to mount an *S-RNase*-independent UI response. Our study was designed based on
398 previous mapping studies of UI in *Solanum* which identified main effect loci for UI on
399 chromosomes 3, 12, and/or 1 (Bernacchi and Tanksley, 1997). Other analyses have confirmed
400 that *ui1.1* is associated with the presence/absence of functional pistil-side *S-RNase*, at least
401 between *Solanum* lineages in which one genotype is SI. The involvement of *S-RNase* for
402 interspecific pollen rejection was confirmed via transformation of SC *Nicotiana* species in which
403 pollen rejection occurred from non transformed SC *Nicotiana* species demonstrating that *S-*
404 *RNase* is sufficient for UI ((Murfett *et al.*, 1996). Nonetheless, because the *S*-locus is a large and
405 genetically complex chromosomal region, additional loci within this region might also contribute
406 to *S-RNase*-independent UI among genotypes that lack *S-RNase* but still show UI phenotypes.
407 Our results, however, do not support the involvement of additional pistil-side loci at *ui1.1* in UI
408 rejection in this particular species pair; we detected no additional effect of *S. pennellii* alleles at
409 *ui1.1* between our two genotypes, both of which lack *S-RNase* function.

410 In contrast to *ui1.1*, our results confirm that *S-RNase*-independent UI is the joint product
411 of *S. pennellii* alleles at chromosomes 3 and 12. Molecular analyses in other *Solanum* species
412 pairs indicate that pistil-side HT protein contributes to the effect associated with *ui12.1* between
413 lineages showing UI. Requirement of HT protein was demonstrated for pollen rejection from *N.*
414 *plumbaginifolia* (Hancock *et al.*, 2003) and within *Solanum* one of the tandemly duplicated HT
415 proteins (HT-A) was detected and expressed for a number of species implicating its function in
416 UI (Covey *et al.*, 2010). In addition, a QTL analysis between *S. lycopersicum* and a different (SI)

bioRxiv preprint doi: https://doi.org/10.1101/094912; this version posted December 24, 2016. The copyright holder for this preprint (which was not certified by peer review) is the author/funder, who has granted bioRxiv a license to display the preprint in perpetuity. It is made available under a CC-BY-NC-ND 4.0 International license.

417 genotype of *S. pennellii* (Jewell, 2016) indicated that presence/absence of HT protein was
418 significantly associated with the strength of the UI response in a segregating F2 population.
419 Although we do not have equivalently direct data on the molecular underpinnings of *ui12.1* here,
420 based on these other studies our working hypothesis is that the effect of IL12-3 on UI is partly or
421 solely due to *S. pennellii* alleles at HT.

422 In comparison to *ui1.1* and *ui12.1*, the molecular loci underpinning *ui3.1* remain
423 unknown, although Jewell (2016) identified several potential genes, and three especially strong
424 candidates, for this locus by combining additional genomic and gene expression data (Pease *et*
425 *al.*, 2016) with the mapped location of *ui3.1* in that study. Interestingly, our findings here suggest
426 that *ui3.1* is more complex than revealed in that and other mapping experiments. QTL analysis
427 has known limitations in terms of identifying number, location, and individual effects of loci
428 because detection depends on the heritability of the trait, the size of the segregating population,
429 and the density of genetic markers (cite). Accordingly, the observation that single QTL can
430 resolve into more than one underlying locus is not uncommon (Mackay *et al.*, 2009), especially
431 when the confidence intervals on this locus are broad. In this case, *ui3.1* was mapped to a region
432 of ~100 cM between *S. pennellii* and *S. lycopersicum* (Jewell, 2016) and ~10 cM between *S.*
433 *habrochaites* and *S. lycopersicum*, (Bernacchi and Tanksley, 1997), both of which could easily
434 harbor >1 contributing locus.

435 Given this, currently the most parsimonious inference from our observations is that (at
436 least) two loci contribute additively to quantitative UI expression at *ui3.1*, one located in the
437 genomic region overlapping between IL3-3 and IL3-4, and one in the region unique to IL3-3 (see
438 Results, and Figure 3B). Nonetheless, there are other alternative interpretations of our
439 observations. For example, tomato chromosomes are known to be enriched for pericentromeric

bioRxiv preprint doi: https://doi.org/10.1101/094912; this version posted December 24, 2016. The copyright holder for this preprint (which was not certified by peer review) is the author/funder, who has granted bioRxiv a license to display the preprint in perpetuity. It is made available under a CC-BY-NC-ND 4.0 International license.

heterochromatin (Wang *et al.*, 2006; Tanksley *et al.*, 1992). Marker delineated breakpoints indicate that IL3-3 overlaps the centromeric region, and therefore contains centromeric heterochromatin from *S. pennellii* that matches the species origin of the rest of the introgression. In comparison, IL3-4 does not contain the *S. pennellii* centromeric region. Given this, it's possible that the phenotypic difference between IL3-3 and IL3-4 is instead due to position effects at *ui3.1* that are associated with proximity to conspecific (IL3-3) versus heterospecific (IL3-4) centromeric heterochromatin. Interestingly, this still implies that two loci are involved in the phenotypic patterns we observed at *ui3.1*, just that the second 'locus' is the regulatory environment associated with species differences in the pericentromeric region.

Regardless, in terms of our goals to evaluate the minimum number of loci required to express pistil-side *S-RNase*-independent UI, and evaluate the relative contribution of three different chromosomal regions to this phenotype, our data indicate that two to three loci at two genomic locations—on chromosomes 3 and 12—are jointly required and sufficient to express this important postmating interspecific barrier.

Source of Transmission Ratio Distortion:

We detected evidence of transmission ratio distortion during the generation of our double introgression lines. One interpretation is that these distorted genotypes are due to gametophytic selection against particular haploid pollen genotypes in the F1 (doubly heterozygous) style in each case. Genetic differences among male gametophytes could result in either differential gametophytic selection or competition, both of which could potentially influence genotype frequencies in the next generation (Snow and Mazer, 1988). For example, gametophytic selection could change the probability of fertilization based on genetic differences expressed in

bioRxiv preprint doi: https://doi.org/10.1101/094912; this version posted December 24, 2016. The copyright holder for this preprint (which was not certified by peer review) is the author/funder, who has granted bioRxiv a license to display the preprint in perpetuity. It is made available under a CC-BY-NC-ND 4.0 International license.

463 the male gametophyte according to a simple model illustrated in Figure 2. In this case, pollen
464 that carries both *S. pennellii* alleles for IL 3-3 and IL 12-3 has a growth or persistence advantage
465 in the heterozygous F1 pistil whereas pollen carrying *S. lycopersicum* alleles is preferentially
466 selected against (Figure 2). This model implies that S. *pennellii*-derived proteins in the style are
467 able to differentially recognize and reject pollen that lacks *S. pennellii* alleles at *ui3.1* and *ui12.1*.
468 This is intriguing because these loci are expected to have pistil-side functions but are not
469 necessarily expected to mediate pollen-side involvement in UI. In contrast, known loci that
470 influence pollen-side expression of UI are located on chromosomes 1, 6, and 10 (Li and Chetelat,
471 2015; Li and Chetelat, 2010; Li *et al.*, 2010; Chetelat and DeVerna, 1991) although these
472 observations do not exclude the potential involvement of additional loci on other chromosomes.
473 We note also that dissimilar patterns of TRD are observed in DIL populations from two other
474 NIL combinations, where some genotypes with *S. pennellii* alleles are significantly
475 underrepresented (Results). In these later cases, however, we cannot exclude the possibility that
476 pollen carrying heterospecific chromosomal segments is simply less viable or less competitive
477 than 'pure' S. *lycopersicum* pollen (i.e. that TRD is due to reduced hybrid male fertility in these
478 genotypes). In addition, patterns of TRD can also be due to other complex causes such as
479 dysfunction (hybrid inviability) in both male and female gametes that results in TRD due to
480 differential (sex independent) gamete survival (Koide *et al.*, 2008) or to differential survival of
481 post-fertilization hybrid zygotes. Therefore, although gametophytic selection might explain part
482 or all of the patterns of TRD we observed, other complex causes are also possible.
483
484 **Unilateral Incompatibly and Reproductive Isolation:**
485 The active recognition and rejection of heterospecific pollen tubes growing within the

bioRxiv preprint doi: https://doi.org/10.1101/094912; this version posted December 24, 2016. The copyright holder for this preprint (which was not certified by peer review) is the author/funder, who has granted bioRxiv a license to display the preprint in perpetuity. It is made available under a CC-BY-NC-ND 4.0 International license.

pistil is a form of postmating cryptic female choice against heterospecific mates. In the Solanaceae, UI is a particularly common reproductive isolating barrier, especially in genera that have both SI and SC species (Bedinger *et al.*, 2011; Lewis and Crowe, 1958). Dissecting the mechanisms that contribute to UI can therefore provide insight into the expression of this reproductive barrier among lineages. Here we have shown that relatively few loci are sufficient to express UI. Moreover, these pistil-side mechanisms likely share genetic components with self-incompatibility mechanisms within species. Previous work has shown that *S-RNase* necessary for SI is also a key pistil-side contributor to UI (Murfett *et al.*, 1996), as is HT (McClure *et al.*, 1999). Moreover, HT appears to contribute to both *S-RNase* dependent and *S-RNase* independent mechanisms of UI among some species (Covey *et al.*, 2010; Tovar−Méndez *et al.*, 2016). Given these dual functions, it is plausible that the molecular machinery for mounting a UI response is already present in the styles of SI species, and its phenotypic expression merely requires encountering heterospecific SC pollen. Nonetheless, the existence of several redundant mechanisms (i.e. *S-RNase* independent and dependent mechanisms) of UI suggests that this heterospecific barrier is not merely a pleiotropic by-product of stylar competence for SI. Indeed, it is possible that the molecular mechanism(s) underlying *ui3.1* are not shared with SI recognition and rejection, consistent with independently selected and maintained mechanisms specifically for UI. Evaluating this possibility awaits further fine-mapping and functional characterization of this locus (or loci) in the future.

bioRxiv preprint doi: https://doi.org/10.1101/094912; this version posted December 24, 2016. The copyright holder for this preprint (which was not certified by peer review) is the author/funder, who has granted bioRxiv a license to display the preprint in perpetuity. It is made available under a CC-BY-NC-ND 4.0 International license.

ACKNOWLEDGMENTS

The authors thank Ashley Huh and C.J. Jewell for data collection and assistance with experimental material. The authors would also like to thank Dean Castillo for advice on statistical analyses. We also thank the Indiana University Bloomington greenhouse staff. Finally, the authors would like to thank X # of reviewers for comments that greatly improved the manuscript. This research was funded by NSF grant MCB-1127059.

bioRxiv preprint doi: https://doi.org/10.1101/094912; this version posted December 24, 2016. The copyright holder for this preprint (which was not certified by peer review) is the author/funder, who has granted bioRxiv a license to display the preprint in perpetuity. It is made available under a CC-BY-NC-ND 4.0 International license.

513 LITERATURE CITED

514 Alonzo, S. H., Stiver, K. A. & Marsh-Rollo, S. E. (2016). Ovarian fluid allows directional
515 cryptic female choice despite external fertilization. *Nature Communications* 7.

516 Baek, Y. S., Covey, P. A., Petersen, J. J., Chetelat, R. T., McClure, B. & Bedinger, P. A. (2015).
517 Testing the SI× SC rule: pollen–pistil interactions in interspecific crosses between
518 members of the tomato clade (Solanum section Lycopersicon, Solanaceae). *American*
519 *Journal of Botany* 102(2): 302-311.

520 Bedinger, P. A., Chetelat, R. T., McClure, B., Moyle, L. C., Rose, J. K., Stack, S. M., van der
521 Knaap, E., Baek, Y. S., Lopez-Casado, G. & Covey, P. A. (2011). Interspecific
522 reproductive barriers in the tomato clade: opportunities to decipher mechanisms of
523 reproductive isolation. *Sexual Plant Reproduction* 24(3): 171-187.

524 Bernacchi, D. & Tanksley, S. D. (1997). An interspecific backcross of Lycopersicon
525 esculentum× L. hirsutum: linkage analysis and a QTL study of sexual compatibility
526 factors and floral traits. *Genetics* 147(2): 861-877.

527 Bernasconi, G., Ashman, T.-L., Birkhead, T., Bishop, J., Grossniklaus, U., Kubli, E., Marshall,
528 D., Schmid, B., Skogsmyr, I. & Snook, R. (2004). Evolutionary ecology of the prezygotic
529 stage. *Science* 303(5660): 971-975.

530 Brown, M. & Lowe, D. G. (2007). Automatic panoramic image stitching using invariant features.
531 *International journal of computer vision* 74(1): 59-73.

532 Canady, M. A., Ji, Y. & Chetelat, R. T. (2006). Homeologous recombination in Solanum
533 lycopersicoides introgression lines of cultivated tomato. *Genetics* 174(4): 1775-1788.

bioRxiv preprint doi: https://doi.org/10.1101/094912; this version posted December 24, 2016. The copyright holder for this preprint (which was not certified by peer review) is the author/funder, who has granted bioRxiv a license to display the preprint in perpetuity. It is made available under a CC-BY-NC-ND 4.0 International license.

534 Castillo, D. M. & Moyle, L. C. (2014). Intraspecific sperm competition genes enforce post-
535 mating species barriers in Drosophila. In *Proc. R. Soc. B*, Vol. 281, 20142050: The Royal
536 Society.
537 Chalivendra, S. C., Lopez-Casado, G., Kumar, A., Kassenbrock, A. R., Royer, S., Tovar-
538 Mèndez, A., Covey, P. A., Dempsey, L. A., Randle, A. M. & Stack, S. M. (2013).
539 Developmental onset of reproductive barriers and associated proteome changes in
540 stigma/styles of Solanum pennellii. *Journal of experimental botany* 64(1): 265-279.
541 Charlesworth, D. & Charlesworth, B. (1979). The evolution and breakdown of S-allele systems.
542 *Heredity* 43(1): 41-55.
543 Chetelat, R. & DeVerna, J. (1991). Expression of unilateral incompatibility in pollen of
544 Lycopersicon pennellii is determined by major loci on chromosomes 1, 6 and 10.
545 *Theoretical and Applied Genetics* 82(6): 704-712.
546 Covey, P. A., Kondo, K., Welch, L., Frank, E., Sianta, S., Kumar, A., Nuñez, R., Lopez-Casado,
547 G., Van Der Knaap, E., Rose, J. K. C., McClure, B. A. & Bedinger, P. A. (2010).
548 Multiple features that distinguish unilateral incongruity and self-incompatibility in the
549 tomato clade. *The Plant Journal* 64(3): 367-378.
550 Cruz-Garcia, F., Hancock, C. N. & McClure, B. A. (2003). S-RNase Complexes and Pollen
551 Rejection. *Journal of Experimental Botany* 54(380): 123-130.
552 de Graaf, B. H. J. (1999). Pistil proline-rich proteins in *Nicotiana tabacum*. Vol. PhD thesis
553 Nijmegen, The Netherlands: Catholic University.
554 de Nettancourt, D. (1977). *Incompatibility in angiosperms.* Heidelberg, Germany: Springer-
555 Verlag.

bioRxiv preprint doi: https://doi.org/10.1101/094912; this version posted December 24, 2016. The copyright holder for this preprint (which was not certified by peer review) is the author/funder, who has granted bioRxiv a license to display the preprint in perpetuity. It is made available under a CC-BY-NC-ND 4.0 International license.

556 Eshed, Y., Abu-Abied, M., Saranga, Y. & Zamir, D. (1992). Lycopersicon esculentum lines
557 containing small overlapping introgressions from L. pennellii. *Theoretical and applied*
558 *genetics* 83(8): 1027-1034.
559 Eshed, Y. & Zamir, D. (1994). A genomic library of Lycopersicon pennellii in L. esculentum: a
560 tool for fine mapping of genes. *Euphytica* 79(3): 175-179.
561 Eshed, Y. & Zamir, D. (1995). An introgression line population of Lycopersicon pennellii in the
562 cultivated tomato enables the identification and fine mapping of yield-associated QTL.
563 *Genetics* 141(3): 1147-1162.
564 Gur, A. & Zamir, D. (2004). Unused natural variation can lift yield barriers in plant breeding.
565 *PLoS Biol* 2(10): e245.
566 Hancock, C. N., Kondo, K., Beecher, B. & McClure, B. A. (2003). The S-locus and Unilateral
567 Incompatibility. *Philosophical Transactions of the Royal Society B: Biological Sciences*
568 358(1434): 1133-1140.
569 Hua, Z. & Kao, T.-h. (2006). Identification and characterization of components of a putative
570 Petunia S-locus F-box–containing E3 ligase complex involved in S-RNase–based self-
571 incompatibility. *The Plant Cell* 18(10): 2531-2553.
572 Jewell, C. P. (2016). Genetics and evolution of reproductive behavior in Solanaceae. Indiana
573 University. PhD Thesis.
574 Koide, Y., Onishi, K., Nishimoto, D., Baruah, A. R., Kanazawa, A. & Sano, Y. (2008). Sex‐
575 independent transmission ratio distortion system responsible for reproductive barriers
576 between Asian and African rice species. *New Phytologist* 179(3): 888-900.

bioRxiv preprint doi: https://doi.org/10.1101/094912; this version posted December 24, 2016. The copyright holder for this preprint (which was not certified by peer review) is the author/funder, who has granted bioRxiv a license to display the preprint in perpetuity. It is made available under a CC-BY-NC-ND 4.0 International license.

577 Kondo, K., Yamamoto, M., Matton, D. P., Sato, T., Hirai, M., Norioka, S., Hattori, T. &
578 Kowyama, Y. (2002). Cultivated tomato has defects in both S‐RNase and HT genes
579 required for stylar function of self‐incompatibility. *The Plant Journal* 29(5): 627-636.
580 Lewis, D. & Crowe, L. (1958). Unilateral interspecific incompatibility in flowering plants.
581 *Heredity* 12: 233-256.
582 Li, W. & Chetelat, R. T. (2010). A pollen factor linking inter-and intraspecific pollen rejection in
583 tomato. *Science* 330(6012): 1827-1830.
584 Li, W. & Chetelat, R. T. (2015). Unilateral incompatibility gene ui1. 1 encodes an S-locus F-box
585 protein expressed in pollen of Solanum species. *Proceedings of the National Academy of*
586 *Sciences* 112(14): 4417-4422.
587 Li, W., Royer, S. & Chetelat, R. T. (2010). Fine mapping of ui6. 1, a gametophytic factor
588 controlling pollen-side unilateral incompatibility in interspecific solanum hybrids.
589 *Genetics* 185(3): 1069-1080.
590 Li, W. T. & Chetelat, R. T. (2014). The Role of a Pollen-Expressed Cullin1 Protein in
591 Gametophytic Self-Incompatibility in Solanum. *Genetics* 196(2): 439-+.
592 Mable, B. K. (2008). Genetic causes and consequences of the breakdown of self-incompatibility:
593 case studies in the *Brassicaceae*. *Genetics Research* 90(01).
594 Mackay, T. F., Stone, E. A. & Ayroles, J. F. (2009). The genetics of quantitative traits:
595 challenges and prospects. *Nature Reviews Genetics* 10(8): 565-577.
596 Manier, M. K., Lüpold, S., Belote, J. M., Starmer, W. T., Berben, K. S., Ala-Honkola, O.,
597 Collins, W. F. & Pitnick, S. (2013). Postcopulatory sexual selection generates speciation
598 phenotypes in Drosophila. *Current Biology* 23(19): 1853-1862.

bioRxiv preprint doi: https://doi.org/10.1101/094912; this version posted December 24, 2016. The copyright holder for this preprint (which was not certified by peer review) is the author/funder, who has granted bioRxiv a license to display the preprint in perpetuity. It is made available under a CC-BY-NC-ND 4.0 International license.

McClure, B., Mou, B., Canevascini, S. & Bernatzky, R. (1999). A small asparagine-rich protein required for S-allele-specific pollen rejection in *Nicotiana*. *Proceedings of the National Academy of Sciences* 96: 13548–13553.

McClure, B. A., Cruz-Garcia, F., Beecher, B. & Sulaman, W. (2000). Factors Affecting Inter- and Intraspecific Pollen Rejection in *Nicotiana*. *Annals of Botany* 85: 113-123.

McClure, B. A., Haring, V., Ebert, P. R., Anderson, M. A., Simpson, R. J., Sakiyama, F. & Clarke, A. E. (1989). Style self-incompatibility gene products of *Nicotlana alata* are ribonucleases. *Nature* 342(6252): 955-957.

Moyle, L. C. (2008). Ecological and evolutionary genomics in the wild tomatoes (Solanum sect. Lycopersicon). *Evolution* 62(12): 2995-3013.

Murfett, J., Strabala, T. J., Zurek, D. M., Mou, B., Beecher, B. & McClure, B. A. (1996). S RNase and interspecific pollen rejection in the genus Nicotiana: multiple pollen-rejection pathways contribute to unilateral incompatibility between self-incompatible and self-compatible species. *The Plant Cell* 8(6): 943-958.

Pease, J. B., Guerrero, R. F., Sherman, N. A., Hahn, M. W. & Moyle, L. C. (2016). Molecular mechanisms of postmating prezygotic reproductive isolation uncovered by transcriptome analysis. *Molecular ecology* 25(11): 2592-2608.

Price, C. S. (1997). Conspecific sperm precedence in Drosophila. *Nature* 388(6643): 663-666.

RStudio Team (2015). RStudio: Integrated Development for R. RStudio, Inc. Boston, MA.

Rutley, N. & Twell, D. (2015). A decade of pollen transcriptomics. *Plant reproduction* 28(2): 73-89.

Schneider, C. A., Rasband, W. S. & Eliceiri, K. W. (2012). NIH Image to ImageJ: 25 years of image analysis. *Nature Methods* 9(7): 671-675.

bioRxiv preprint doi: https://doi.org/10.1101/094912; this version posted December 24, 2016. The copyright holder for this preprint (which was not certified by peer review) is the author/funder, who has granted bioRxiv a license to display the preprint in perpetuity. It is made available under a CC-BY-NC-ND 4.0 International license.

622 Snow, A. A. & Mazer, S. J. (1988). Gametophytic selection in Raphanus raphanistrum: a test for
623 heritable variation in pollen competitive ability. *Evolution*: 1065-1075.
624 Stone, J. L. (2002). Molecular Mechanisms Underlying The Breakdown Of Gametophytic Self-
625 incompatibility. *The Quarterly Review of Biology* 77(1): 17-32.
626 Takayama, S. & Isogai, A. (2005). Self-incompatibility in Plants. *Annual Review of Plant*
627 *Biology* 56(1): 467-489.
628 Tanksley, S., Ganal, M., Prince, J., De Vicente, M., Bonierbale, M., Broun, P., Fulton, T.,
629 Giovannoni, J., Grandillo, S. & Martin, G. (1992). High density molecular linkage maps
630 of the tomato and potato genomes. *Genetics* 132(4): 1141-1160.
631 Tao, R. & Iezzoni, A. F. (2010). The S-RNase-based gametophytic self-incompatibility system in
632 *Prunus* exhibits distinct genetic and molecular features. *Scientia Horticulturae* 124(4):
633 423-433.
634 Tovar-Méndez, A., Kumar, A., Kondo, K., Ashford, A., Baek, Y. S., Welch, L., Bedinger, P. A.
635 & McClure, B. A. (2014). Restoring pistil-side self-incompatibility factors recapitulates
636 an interspecific reproductive barrier between tomato species. *The Plant Journal* 77: 727-
637 736.
638 Tovar‐Méndez, A., Lu, L. & McClure, B. (2016). HT proteins contribute to S‐RNase‐
639 independent pollen rejection in Solanum. *The Plant Journal*.
640 Wang, Y., Tang, X., Cheng, Z., Mueller, L., Giovannoni, J. & Tanksley, S. D. (2006).
641 Euchromatin and pericentromeric heterochromatin: comparative composition in the
642 tomato genome. *Genetics* 172(4): 2529-2540.

bioRxiv preprint doi: https://doi.org/10.1101/094912; this version posted December 24, 2016. The copyright holder for this preprint (which was not certified by peer review) is the author/funder, who has granted bioRxiv a license to display the preprint in perpetuity. It is made available under a CC-BY-NC-ND 4.0 International license.

643 Zhao, L., Huang, J., Zhao, Z. H., Li, Q., Sims, T. L. & Xue, Y. B. (2010). The Skp1-like protein
644 SSK1 is required for cross-pollen compatibility in S-RNase-based self-incompatibility.
645 *Plant Journal* 62(1): 52-63.

646

647

bioRxiv preprint doi: https://doi.org/10.1101/094912; this version posted December 24, 2016. The copyright holder for this preprint (which was not certified by peer review) is the author/funder, who has granted bioRxiv a license to display the preprint in perpetuity. It is made available under a CC-BY-NC-ND 4.0 International license.

Table 1. Proportion of pollen tube growth for each genotype with upper (upr) and lower (lwr) 95% confidence intervals.

Genotype (Female x Male)	Mean ± SE	CI.95.lwr	CI.95.upr	# of biological replicates
NIL 1-1	0.9398 ± 0.0154	0.8650	1.0144	3
NIL 3-3	0.9369 ± 0.0328	0.8621	1.011	3
NIL 3-4	0.9233 ± 0.0402	0.8681	1.002	4
NIL 12-3	0.9785 ± 0.0117	0.9206	1.036	5
DIL 1-1 x 12-3	0.8459 ± 0.0200	0.7811	0.9105	4
DIL 12-3 x 3-3	0.5082 ± 0.0317	0.4693	0.5987	4
DIL 3-4 x 12-3	0.7609 ± 0.0472	0.7080	0.8136	6

bioRxiv preprint doi: https://doi.org/10.1101/094912; this version posted December 24, 2016. The copyright holder for this preprint (which was not certified by peer review) is the author/funder, who has granted bioRxiv a license to display the preprint in perpetuity. It is made available under a CC-BY-NC-ND 4.0 International license.

Table 2A. Observed and expected (in parentheses) genotype frequencies for the crosses between chromosome region 12-3 (female) and chromosome region 3-3 (male) deviate from expected values, X^2 (8, N = 26) = 51.217, p-value = 2.38e-08. Genotypes that are overrepresented are indicated by +, after Bonferroni correction.

	Genotype at IL 12-3		
Genotype at IL 3-3	**LL**	**LP**	**PP**
LL	1 (1.63)	1 (3.25)	1 (1.63)
LP	0 (3.25)	2 (6.5)	13 (3.25)$^{+}$
PP	1 (1.63)	1 (3.25)	6 (1.63)$^{+}$

Table 2B. Observed and expected (in parentheses) genotype frequencies for the crosses between chromosome region 3-4 (female) and chromosome region 12-3 (male) deviate from expected values X^2 (8, N= 117) = 25.86, p-value = 0.001103. Genotypes that are underrepresented are indicated by **-,** after Bonferroni correction.

	Genotype at IL 3-4		
Genotype at IL 12-3	**LL**	**LP**	**PP**
LL	14 (7.31)	15 (14.63)	11 (7.31)
LP	18 (14.63)	23 (29.25)	23 (14.63)
PP	4 (7.31)	3 (14.63)$^{-}$	6 (7.31)

Table 2C. Observed and expected (in parentheses) genotype frequencies for the crosses between chromosome region 12-3 (female) and chromosome region 1-1 (male) deviate from expected values, X^2 (8, N= 67) = 19.649, p-value = 0.0012. Genotypes that are underrepresented are indicated by **-,** after Bonferroni correction.

	Genotype at IL 12-3		
Genotype at IL 1-1	**LL**	**LP**	**PP**
LL	9 (4.18)	13 (8.375)	7 (4.18)
LP	10 (8.375)	17 (16.75)	5 (8.375)
PP	2 (4.18)	1 (8.375)$^{-}$	3 (4.18)

bioRxiv preprint doi: https://doi.org/10.1101/094912; this version posted December 24, 2016. The copyright holder for this preprint (which was not certified by peer review) is the author/funder, who has granted bioRxiv a license to display the preprint in perpetuity. It is made available under a CC-BY-NC-ND 4.0 International license.

668 FIGURE LEGENDS

669 Figure 1. A) Representative images of the presence (A) and absence (B) of a UI pollen rejection
670 response in the pistil. The white bar is the 1 cm scale used for measuring each style. A) Here, UI
671 is illustrated with the phenotype observed in DIL 3-4 x 12-3, in which pollen rejection occurs
672 approximately three-fourths down the length of the style. The arrowhead indicates where the
673 majority of pollen tubes halt within the female reproductive tract (pistil) in this genotype. B)
674 Compatible cross in which pollen tubes successfully reach the ovary, illustrated with the
675 phenotype observed for NIL 3-4.

676

677 Figure 2. One model of gametophytic selection on different haploid pollen genotypes that could
678 result in transmission ratio distortion among F2s. Two loci (*ui3.1* and *ui12.1*) are designated by
679 whether they have alleles from *S. pennellii* (i.e., 3_P and 12_P) or *S. lycopersicum* (i.e., 3_L and 12_L).
680 Left side: When two NILs are crossed ($3_P3_P\ 12_L12_L$ x $3_L3_L12_P12_P$), the F_1 is heterozygous at the
681 two regions ($3_P\ 12_L\ 3_L12_P$). Selfing this F_1 produces four different haploid pollen genotypes:
682 3_L12_L, 3_L12_P, 3_P12_L, and 3_P12_L. Right side: Based on the genotype of our heterozygous F_1
683 individual ($3_P\ 12_L\ 3_L12_P$) preferential pollen use, and stylar selection against specific pollen
684 genotypes (e.g., 3_L12_L, 3_L12_P, and 3_P12_L), could generate deviations from expected Mendelian
685 ratios.

686

687 Figure 3: Proportion of pollen tube growth by genotypic class. A) Mean value with upper and
688 lower 95% confidence intervals for distance traveled through the length of the style for each
689 genotypic class. The top of the graph (0) represents the stigma, where pollen is placed. The

bioRxiv preprint doi: https://doi.org/10.1101/094912; this version posted December 24, 2016. The copyright holder for this preprint (which was not certified by peer review) is the author/funder, who has granted bioRxiv a license to display the preprint in perpetuity. It is made available under a CC-BY-NC-ND 4.0 International license.

690 bottom of the graph (1.0) represents the ovary, which is at the base of the style. B) The estimated

691 effect size of the two loci (*ui3.1.1*, *ui3.1.2*) inferred to underlie *ui3.1* (see text).

692

693

bioRxiv preprint doi: https://doi.org/10.1101/094912; this version posted December 24, 2016. The copyright holder for this preprint (which was not certified by peer review) is the author/funder, who has granted bioRxiv a license to display the preprint in perpetuity. It is made available under a CC-BY-NC-ND 4.0 International license.

Supplemental Table 1. Near isogenic line accessions used in this study. Accession numbers are from the Tomato Genetics Resource Center (tgrc.ucdavis.edu).

Accession	Introgression Line	n*
LA 4028	IL 1-1	3
LA 3488	IL 3-3	3
LA 4046	IL 3-4	4
LA 4100	IL 12-3	5

* Number of biological replicates per accession

bioRxiv preprint doi: https://doi.org/10.1101/094912; this version posted December 24, 2016. The copyright holder for this preprint (which was not certified by peer review) is the author/funder, who has granted bioRxiv a license to display the preprint in perpetuity. It is made available under a CC-BY-NC-ND 4.0 International license.

698 Supplemental Table 2. CAPs markers used for genotyping with marker ID based on Solgenomics
699 markers.

Ch	cM	Marker ID	Enzyme*	PCR Fragment	L Fragment	P Fragment
1	30.20	C2_At3g06580	*Dpn*II	300	170	270
1	40.00	C2_At4g30890	*Taq*I	600	300+200	350+200
1	58.00	C2_At1g48050	*Taq*I	920	920	750
3	72.40	C2_At3g02910	*Taq*I	450	150	325
3	101.50	C2_At3g47990	*Hae*III	1100	1100	780+320
3	113.00	C2_At1g74520	*Rsa*I	1350	410+390	1350
3	120.50	C2_At5g62440	*Dra*I	950	700	570
3	128.50	C2_At3g47640	*Xba*I	850	850	550+300
12	52.00	T1736	LP*	-	1200	1050
12	74.00	T0801	*Acc*I	589	400	600

700 Ch = chromosome, cM = centiMorgans, * LP is a linked polymorphism (i.e. size difference noticeable after first
701 PCR reaction so no digestion via restriction enzymes necessary), L Frag = Expected size if double homozygous *S.*
702 *lycopersicum*, P Frag = Expected Size if *S. pennellii*

bioRxiv preprint doi: https://doi.org/10.1101/094912; this version posted December 24, 2016. The copyright holder for this preprint (which was not certified by peer review) is the author/funder, who has granted bioRxiv a license to display the preprint in perpetuity. It is made available under a CC-BY-NC-ND 4.0 International license.

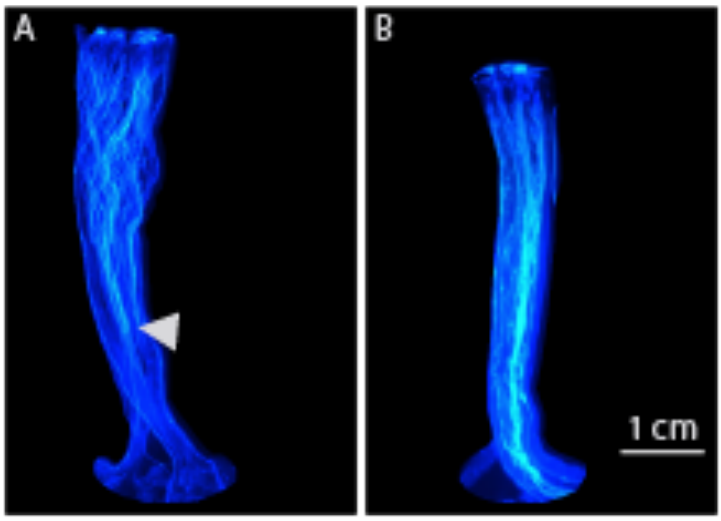
703 Supplemental Figure Legend

704 Supplemental Figure 1. Representative images of the softened and stained pollinated styles,
705 showing proportion of pollen tube growth towards the ovary for each genotype evaluated. White
706 scale bars are 1000 μm.

707

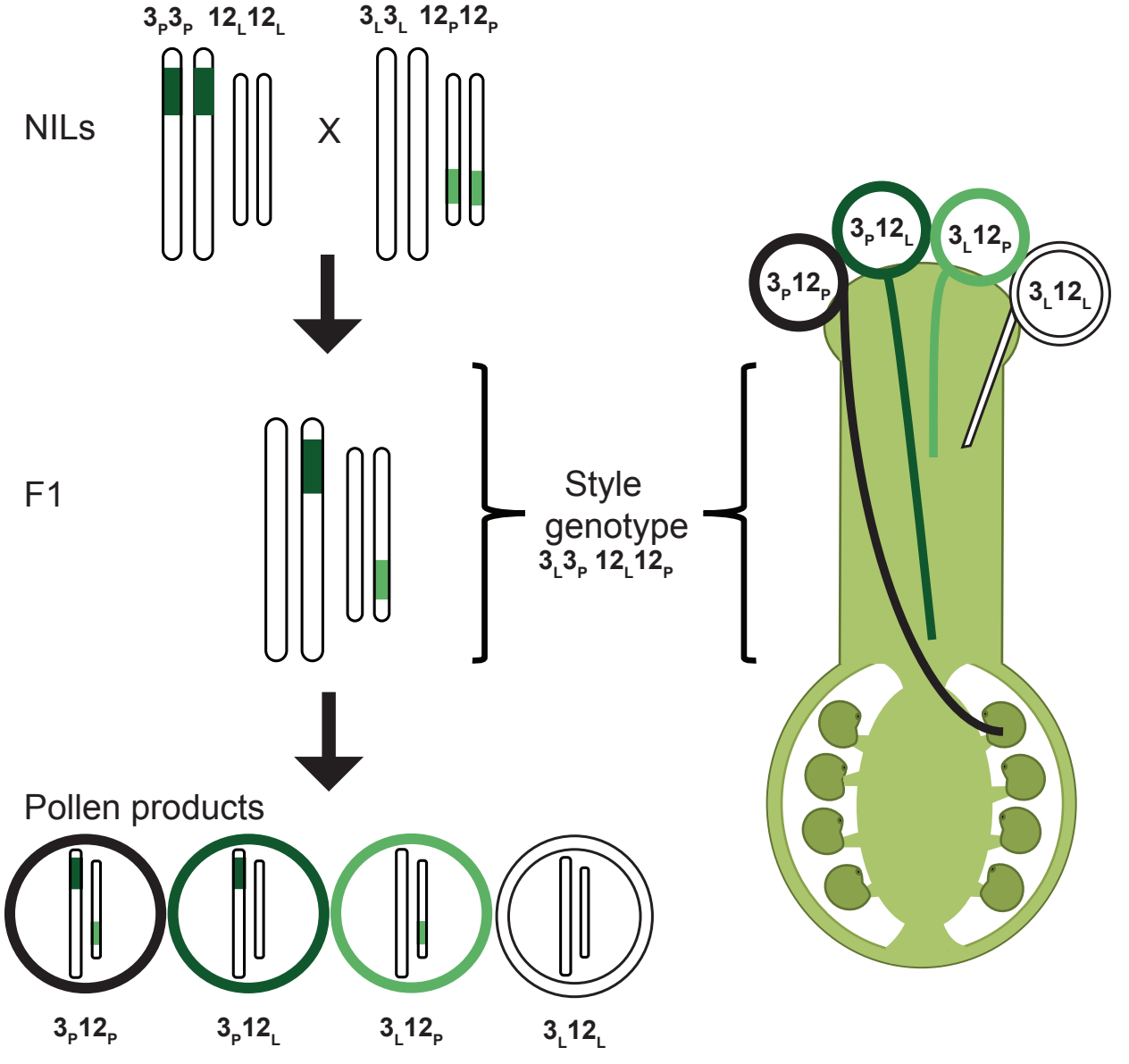
708 Supplemental Figure 2. The relative locations, and overlapping and non-overlapping introgressed
709 regions, for IL 3-3 and IL 3-4 on chromosome 3. Markers locations used for genotyping are
710 illustrated on the right; a single marker identifies either IL 3-3 (marker 72.40) or IL 3-4 (marker
711 128.50), while the three intervening markers fall within the overlapping region. Map generated
712 based on map distances obtained from Solgenomics.net.

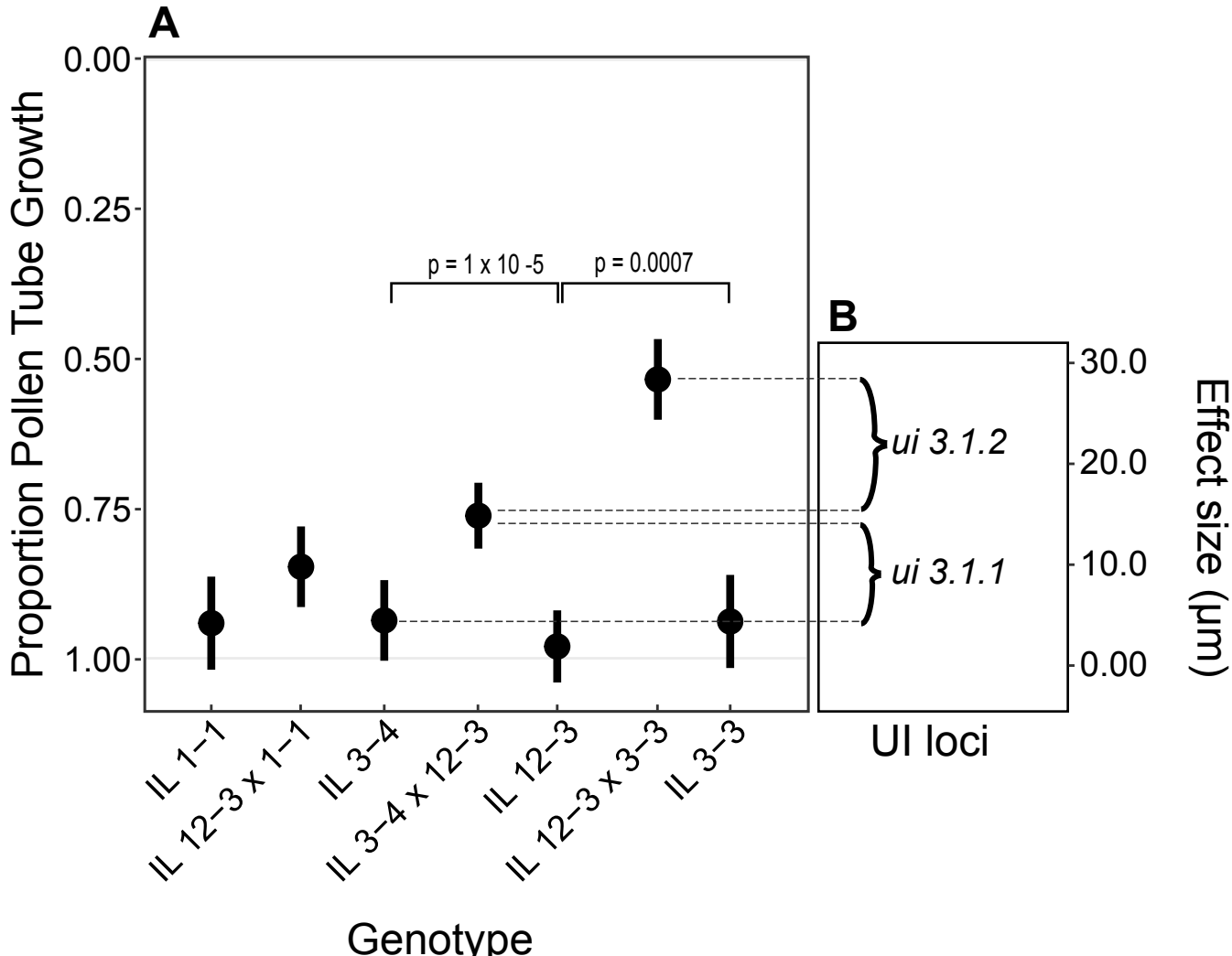
bioRxiv preprint doi: https://doi.org/10.1101/094912; this version posted December 24, 2016. The copyright holder for this preprint (which was not certified by peer review) is the author/funder, who has granted bioRxiv a license to display the preprint in perpetuity. It is made available under a CC-BY-NC-ND 4.0 International license.



713

714


3_P3_P 12_L12_L
3_L3_L 12_P12_P
NILs
X
F1
Style genotype
3_L3_P 12_L12_P
Pollen products
3_P12_P
3_P12_L
3_L12_P
3_L12_L
3_P12_L
3_L12_P
3_P12_P
3_L12_L


A
B
0.00
0.25
0.50
0.75
1.00
Proportion Pollen Tube Growth
p = 1 x 10 -5
p = 0.0007
IL 1–1
IL 12–3 x 1–1
IL 3–4
IL 3–4 x 12–3
IL 12–3
IL 12–3 x 3–3
IL 3–3
Genotype
ui 3.1.2
ui 3.1.1
UI loci
30.0
20.0
10.0
0.00
Effect size (µm)